Evaluation of a combination tumor treatment using thermo-triggered liposomal drug delivery and carbon ion irradiation

Kokuryo, Daisuke ; Aoki, Ichio ; Yuba, Eiji ; Kono, Kenji ; Aoshima, Sadahito ; Kershaw, Jeff ; Saga, Tsuneo

(Citation)
Translational Research,185:24-33

(Issue Date)
2017-07

(Resource Type)
journal article

(Version)
Version of Record

(URL)
https://hdl.handle.net/20.500.14094/90004918

Evaluation of a combination tumor treatment using thermo-triggered liposomal drug delivery and carbon ion irradiation

DAISUKE KOKURYO, ICHIO AOKI, EIJI YUBA, KENJI KONO, SADAHITO AOSHIMA, JEFF KERSHAW, and TSUNEO SAGA

CHIBA, KOBE, HYOGO, SAKAI, AND OSAKA, JAPAN

The combination of radiotherapy with chemotherapy is one of the most promising strategies for cancer treatment. Here, a novel combination strategy utilizing carbon ion irradiation as a high–linear energy transfer (LET) radiotherapy and a thermo-triggered nanodevice is proposed, and drug accumulation in the tumor and treatment effects are evaluated using magnetic resonance imaging relaxometry and immunohistology (Ki-67, n = 15). The thermo-triggered liposomal anticancer nanodevice was administered into colon-26 tumor-grafted mice, and drug accumulation and efficacy was compared for 6 groups (n = 32) that received or did not receive the radiotherapy and thermo trigger. In vivo quantitative R_1 maps visually demonstrated that the multimodal thermosensitive polymer-modified liposomes (MTPLs) can accumulate in the tumor tissue regardless of whether the region was irradiated by carbon ions or not. The tumor volume after combination treatment with carbon ion irradiation and MTPLs with thermo-triggering was significantly smaller than all the control groups at 8 days after treatment. The proposed strategy of combining high-LET irradiation and the nanodevice provides an effective approach for minimally invasive cancer treatment. (Translational Research 2017;185:24–33)

Abbreviations: LET = linear energy transfer; DDS = drug delivery system; MTPL = multimodal thermosensitive polymer-modified liposome; MR = magnetic resonance; MRI = magnetic resonance imaging; IMRT = intensity-modulated radiation therapy; DNA = deoxyribonucleic acid; PEG = polyethylene glycol; $MnSO_4$ = manganese sulfate; EYPC = egg-yolk phosphatidylcholine; DOPE = dioleoylphosphatidylethanolamine; ODVE = octadecyl vinyl ether; EOEOVE = 2-(2-ethoxy)ethoxyethyl vinyl ether; SOBP = spread-out Bragg peak; HIMAC = heavy ion medical accelerator in Chiba; TR = repetition time; TE = echo time; FOV = field of view; NEX = number of averages; T_1 = longitudinal relaxation time; RARE = rapid acquisition with relaxation enhancement; RAREVTR = variable repetition and echo time RARE sequence; ANOVA = analysis of variance; R_1 = longitudinal relaxation rate; Gy = gray; RBE = relative biological effectiveness; DOX = doxorubicin; RNA = ribonucleic acid

From the National Institute of Radiological Sciences (NIRS), National Institutes for Quantum and Radiological Science and Technology (QST), Chiba, Japan; Graduate School of System Informatics, Kobe University, Kobe, Hyogo, Japan; Graduate School of Engineering, Osaka Prefecture University, Sakai, Osaka, Japan; Graduate School of Science, Osaka University, Osaka, Japan.

Submitted for publication March 19, 2016; revision submitted April 12, 2017; accepted for publication April 13, 2017.

Reprint requests: Ichio Aoki, National Institute of Radiological Sciences (NIRS), National Institutes for Quantum and Radiological Science and Technology (QST), 4-9-1 Anagawa, Inage-ku, Chiba, 263-8555, Japan; e-mail: aoki.ichio@qst.go.jp.

1931-5244

http://dx.doi.org/10.1016/j.trsl.2017.04.001

AT A GLANCE COMMENTARY

Kokuryo D, et al.

Background

The combination of radiotherapy with chemotherapy is one of the most promising strategies for cancer treatment. Here, a novel combination strategy utilizing carbon ion irradiation as a high–linear energy transfer (LET) radiotherapy and a thermo-triggered nanodevice is proposed, and drug accumulation in the tumor and treatment effects are evaluated using magnetic resonance imaging (MRI) relaxometry and immunohistology (Ki-67, n = 15).

Translational Significance

In vivo quantitative R_1-maps visually demonstrated that the multimodal thermosensitive polymer-modified liposomes (MTPLs) can accumulate in the tumor tissue regardless of whether the region was irradiated by carbon ions or not. The tumor volume after combination treatment with carbon ion irradiation and MTPLs with thermo-triggering was significantly smaller than all the control groups at 8 days after treatment. The proposed strategy combining high-LET irradiation and the nanodevice provides an effective approach for minimally invasive cancer treatment.

INTRODUCTION

The combination of radiotherapy and chemotherapy, known as chemoradiotherapy, is one of the most common strategies for cancer treatment.[1] Recent technological advances in both radiotherapy and chemotherapy have the potential to further improve tumor treatment. For example, intensity-modulated radiation therapy has been developed for better control of radiation doses in accordance with tumor shape and position.[2,3] Intensity-modulated radiation therapy has been applied to optimize cancer treatments in lung,[4,5] breast,[6-8] and prostate.[9,10] As another example, high–linear energy transfer (LET) particle therapy using protons and heavy ions, in particular carbon ions, has been developed for more precise and confined irradiation.[11] A heavy-ion beam directly causes DNA double-strand break so that apoptotic and necrotic death of tumor cells is induced.[12] Thus, heavy-ion beams have the potential to improve the treatment for hypoxic and/or radiation-resistant tumors. At our institute (National Institute of Radiological Sciences, NIRS), clinical treatment using a carbon-ion beam began in 1994 and by 2014 over 8000 patients have been treated.[11,13] Advances in beam-line technology have allowed tumors in tissues such as lung,[14] head and neck,[15,16] and prostate[17] to be targeted with carbon ions. The combination therapies with carbon-ion irradiation and chemotherapy also were performed.[13,18] However, carbon-ion radiotherapy cannot be applied to the metastatic phase of cancer growth because the total required irradiation dose exceeds safety limits. Thus, for carbon-ion radiotherapy to be most effective it is necessary to combine it with additional treatment strategies.

With regards to advances in chemotherapy, several nanoparticle-based drug carriers, such as micelles, liposomes, and dendrimers, have been developed to increase the efficiency of drug accumulation in tumor and to minimize side-effects.[19,20] Several nanoparticles that have prolonged half-life in the bloodstream show higher passive accumulation in tumor tissues, which is a phenomenon known as the enhanced permeability and retention effect.[21] PEGylated liposomal doxorubicin (DOXIL/Caelyx, Janssen Pharmaceutical, Inc., Titusville, N.J.) has been used clinically to treat ovarian cancer and Kaposi sarcoma. Micelles that incorporate cisplatin (NC6004, Nanocarrier, Japan),[22,23] paclitaxel (NK105, Nihon-Kayaku, Japan),[24,25] and epirubicin (NC6300, Nanocarrier, Kowa, Japan)[26,27] have also been evaluated in clinical trials. However, accumulation of these nanoparticles in the tumor region cannot be monitored and evaluated in vivo. Recently, a number of research groups have developed theranostic nanoparticles that contain both therapeutic drugs for treatment and contrast agents that aid visualization of drug distribution with an in vivo imaging modality or a window chamber system.[28-32] In previous work, we investigated the multimodal thermosensitive polymer-modified liposomes (MTPLs) containing $MnSO_4$ as an magnetic resonance (MR) contrast agent, rhodamine as a fluorescence dye, and doxorubicin (DOX) as an anticancer drug and as a possible theranostic tool.[30] It was found that the transformation of the thermosensitive polymer when heated to over 41°C allows the contents of the MTPLs to be released. MTPL accumulation in the tumor region can also be visualized with MRI and fluorescence imaging, and treatment effects after heating increased significantly.

Previously, conventional radiotherapy combined with a PEGylated nano-drug delivery system (DDS) was reported to enhance treatment efficacy as increases in tumor size were controlled and survival duration was prolonged.[33-36] Although in vitro studies for the proton beam radiotherapy combined with temperature-sensitive liposomes has been reported,[37,38] there is no in vivo report of a high-LET beam radiotherapy, such as a charged proton or carbon beam, combined with nano-DDS therapy. There is also no report of a combined therapy using

radiotherapy and a triggered nano-DDS to induce more localized drug-release. The aim of this article was to evaluate (1) whether accumulation of liposomal nano-DDS in tumor is affected by the high-LET beam radiotherapy, and (2) whether the therapeutic effect is maintained. Here, the performance of MTPL accumulation in the tumor region, regardless of whether the high-LET beam was irradiated before or after administration, was evaluated using preclinical MRI. The treatment efficacy of high-LET irradiation and MTPLs after heating was also evaluated through comparison with a number of control treatment groups.

MATERIALS AND METHODS

Animal and cell line preparation. Forty-seven 6- to 8-week old female BALB/c nude mice (Japan SLC, Shizuoka, Japan and CLEA Japan, Tokyo, Japan) were used for the experiments. The mice were maintained in accordance with the guidelines of NIRS, and all experiments were reviewed and approved by the institute's committee for care and use of laboratory animals.

Colon-26 murine rectal cancer cells were obtained from the RIKEN BioResource Center (Tsukuba, Japan). The cells were maintained in Dulbecco's modified Eagle's medium (Sigma-Aldrich, St Louis, Mo.) supplemented with 10 % fetal bovine serum and incubated in a humidified atmosphere of 5 % CO_2 in air at 37°C. After suspension in phosphate-buffered saline, the cells were subcutaneously grafted (1.0×10^6 cells/50 μl) into both the left and right flanks of the mice, and allowed to grow for 8–10 days before the treatments were applied.

MTPLs. The MTPLs contained $MnSO_4$ as an MR contrast agent, rhodamine as a fluorescence dye, and DOX as an anticancer drug. The MTPL membrane was composed of egg-yolk phosphatidylcholine, dioleoylphosphatidylethanolamine, cholesterol, N-(carbonyl-methoxy polyethylene glycol 2000)-1,2-distearoyl-sn-glycero-3-phosphoethanolamine (PEG2000-DSPE), block copolymer of octadecyl vinyl ether (ODVE), and 2-(2-ethoxy)ethoxyethyl vinyl ether (EOEOVE; poly(EOEOVE)-OD_9), which is a thermosensitive moiety and changes from hydrophilic to hydrophobic at around 41°C, and L-α-phosphatidylethanolamine-N-(lissamine rhodamine B sulfonyl) (ammonium salt) (egg-transphosphatidylated, chicken) (Rhodamine-PE). The ratio of each material was egg-yolk phosphatidylcholine/dioleoylphosphatidylethanolamine/Cholesterol/N-(carbonyl-methoxy polyethylene glycol 2000)-1,2-distearoyl-sn-glycero-3-phosphoethanolamine/poly(EOEOVE)-OD_9/Rhodamine-PE = 23.4/54.6/15/4/2/1. The $MnSO_4$ and DOX were encapsulated in the MTPLs. Detailed procedures for MTPL preparation have been reported previously.[29,30,39,40] The $MnSO_4$ and DOX in the MTPLs release after heating to 41°C, and the MR signal near the heated area is expected to increase in vivo.[30] The characteristics of the MTPLs, such as size and tumor accumulation, have been investigated in previous articles.[30,40] We confirmed that the size of the MTPLs was approximately 100 nm, which is a size suitable for accumulation in the tumor region via the enhanced permeability and retention effect.[21] It was also verified that the MTPLs accumulate in the tumor region for up until 12 hours after the administration with MRI and fluorescence imaging.

Carbon-ion irradiation. Carbon-12 ions were accelerated to 290 MeV/n, 6.0 cm spread-out Bragg peak by the Heavy Ion Medical Accelerator in Chiba (HIMAC) at NIRS. Details about beam characterization and biological irradiation procedures have been described elsewhere.[41] For the present study, the tumor in the left leg was irradiated with the carbon ions at a dose of 5 Gy. The irradiated area was restricted to 1.0×1.0 cm^2 using a collimator to prevent the irradiation of normal tissues around the tumor. Radiation power was optimized so that the Bragg peak was in the center of the tumor.

Experimental design. Details of the experimental design are shown in Fig 1. We defined day 0 to be the date of carbon-ion irradiation, MTPL administration and heating. The 47 mice were separated for 2 groups of experiments: (A) in vivo evaluation of MR signal changes and tumor growth (n = 32, Fig 1*A*), and (B) immunohistological evaluation (n = 15, Fig 1*B*). Six different treatment strategies were applied: heating after carbon-ion irradiation and MTPL administration ("carbon-ion + MTPL + heat"), no treatment for the mouse ("untreated"), carbon-ion irradiation only ("carbon-ion"), carbon-ion irradiation before MTPL administration ("carbon-ion + MTPL"), carbon-ion irradiation after MTPL administration ("MTPL + carbon-ion"), and heating after carbon-ion irradiation without MTPL administration ("carbon-ion + heat").

When appropriate, the MTPLs (0.2 ml, stock solution, with a liquid concentration of over 10 mM) were administered into the tumor model mice from the tail vein at around 10 minutes before or after carbon-ion irradiation. Breaking of the MTPLs was triggered by heating the tumor region to 42.5°C for 10 minutes using a home-made warm water circulation system at around 3 hours after carbon-ion irradiation. The heating system included a thermally conductive gel pad (6 mm in diameter, approximately 45°C, αGEL, Taica, Japan), attached to a hot water circulating silicon tube, which was placed on the surface of the tumor. The pad completely covered a grafted tumor. The temperature in the tumor during heating was measured using a thermocouple controller system (E5CN, Omron, Kyoto,

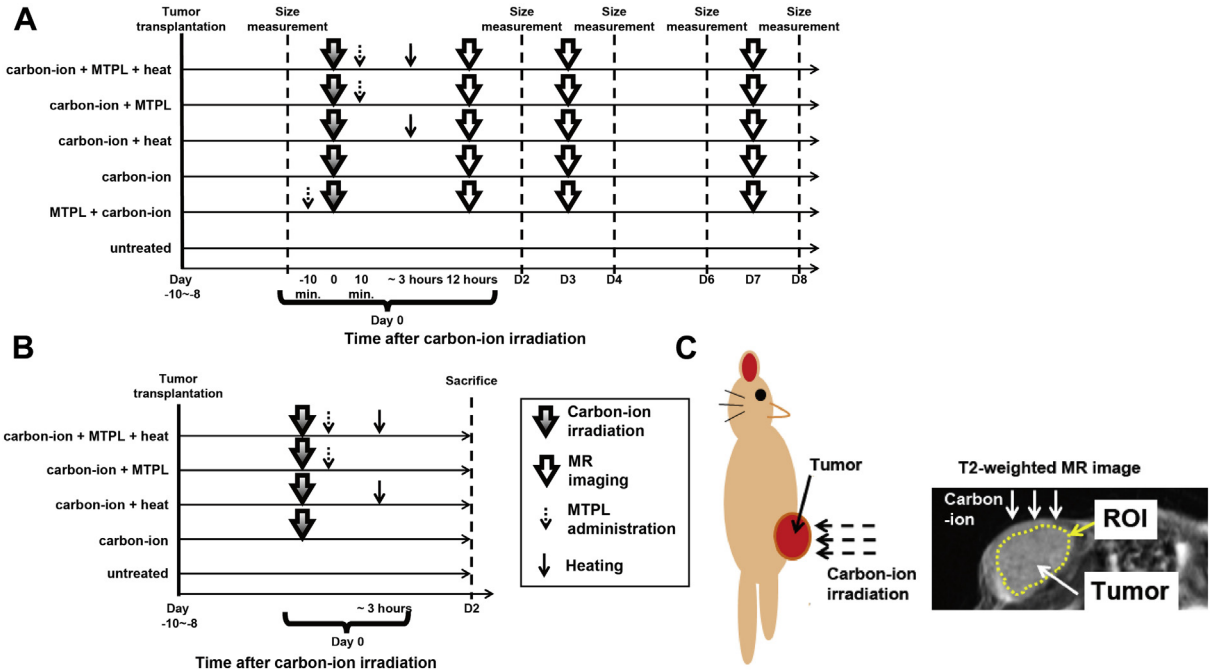

Fig 1. Experimental design for the treatment strategies. **A,** The schedule for treatment with carbon-ion irradiation, MTPLs, and heating is shown. The timing of MR imaging and tumor size measurement is also included. **B,** The schedule for histological evaluation of treatment effects. **C,** The carbon-ion irradiated region and region of interest in the tumor. The carbon-ion irradiation was applied to the tumor on the left flank of the mice (left). The region of interest (dashed yellow circle) use to measure MR signal changes was set in the tumor as shown on the right MR image. MR, magnetic resonance; MTPL, multimodal thermosensitive polymer-modified liposome.

Japan), with the thermocouple probe inserted under the skin into the subcutaneous tumor. Temperature changes in the tumor were monitored during heating, and the pad was put on or removed from the tumor manually when the temperature reached 42.5°C.

Evaluation of MTPL accumulation using MRI. Three mice from each treatment strategy in group A (except for the "untreated" group) were selected for MR imaging to evaluate whether the carbon-ion irradiation influences MTPL accumulation in the tumor or not. MR images were acquired at 12 hours, 3 days, and 7 days after the treatments.

MR imaging was performed using a 7.0 Tesla preclinical, 40-cm bore magnet (Kobelco, Kobe, Japan and Jastec, Kobe, Japan) interfaced to an AVANCE I system (Bruker-Biospin, Ettlingen, Germany) with a 35-mm diameter volume coil for transmission and reception (RAPID Biomedical, Lymper, Germany). During MRI measurement, body temperature was measured using an optical fiber thermometer (FOT-M, FISO Technology Inc., Quebec, Canada) inserted into the rectum, and maintained at approximately 36.5 ± 0.5°C by an automatic homemade warm-air heating system. The mice were anesthetized with 1.5%–2.0 % isoflurane (Escain, Mylan Co. Ltd., Tokyo, Japan) gas and a 1:2 O_2:room-air mixture.

Multi-slice T_1-weighted images were acquired using a conventional spin-echo sequence with the following parameters: repetition time (TR) = 400 ms; echo time (TE) = 9.6 ms; field-of-view = 38.4 × 19.2 mm^2; number of slices = 9; slice thickness = 1.0 mm; slice gap = 0.5 mm; matrix = 256 × 128, and number of averages = 4. For quantitative T_1 measurement, a variable repetition and echo time RARE sequence that acquires multi-TR and multi-TE data was used with the following parameters; TR = 5000, 3000, 1500, 800, 400, and 200 ms; TE = 11, 33, 55, 77, and 99 ms; RARE factor = 2; number of slices = 1; number of averages = 1. Other parameters were the same as for the T_1-weighted images. The slice position was set at the center slice from the T_1-weighted images.

In vivo tumor growth. To evaluate in vivo tumor growth at the irradiated site, the 32 mice of group A were separated for the "carbon-ion + MTPL + heat" treatment strategy (n = 5), and 5 control strategies: "untreated" (n = 7), "carbon-ion" (n = 6), "carbon-ion + MTPL" (n = 5), "MTPL + carbon-ion" (n = 4), and "carbon-ion + heat" (n = 5). The lengths of the long and short axes and the depth of the tumor were measured using a vernier caliper. Tumor volume was calculated with the formula: tumor volume = (long axis) × (short

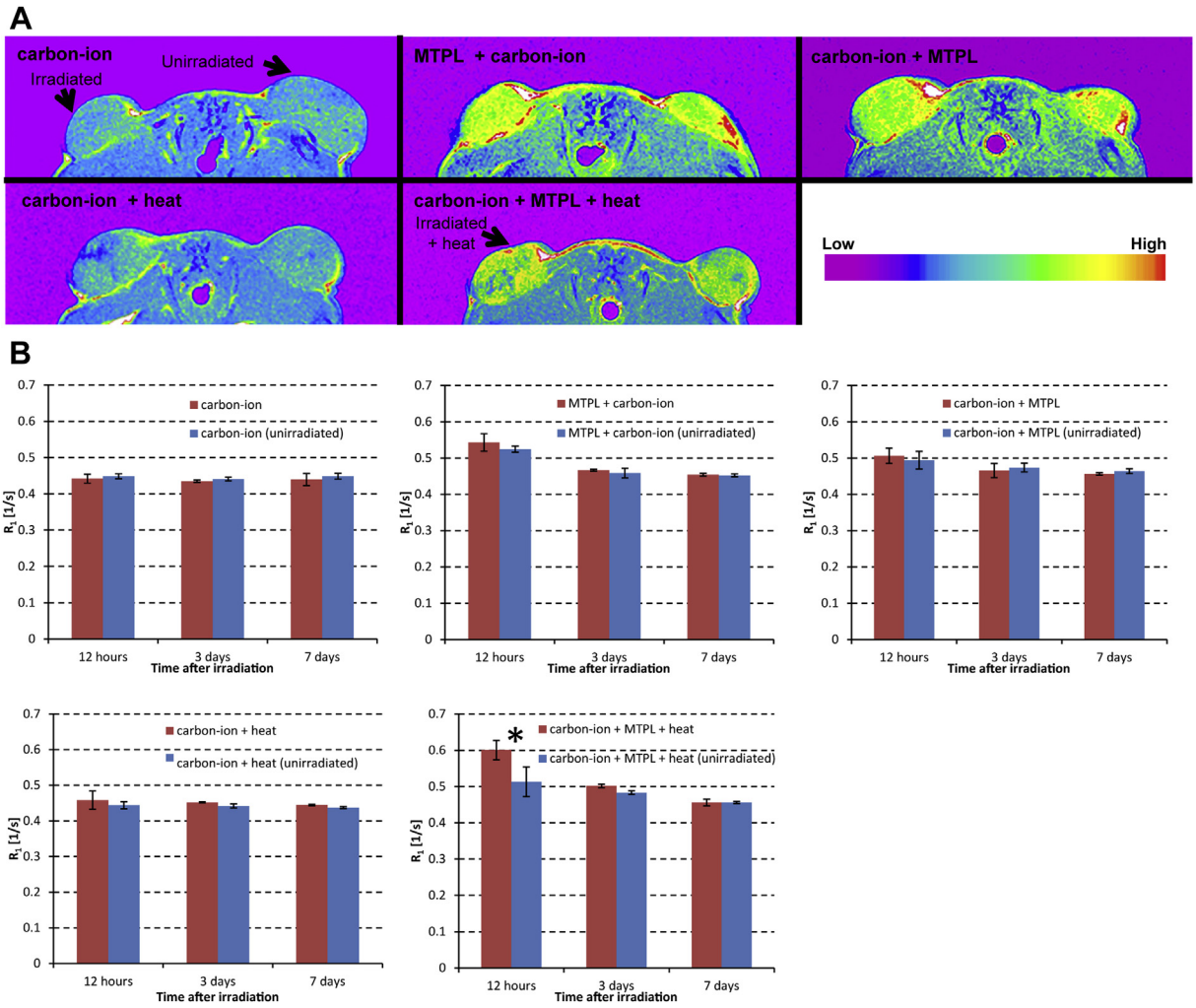

Fig 2. In vivo MR imaging after MTPL administration. **A,** Typical T_1-weighted MR images at 12 hours after treatment for each treatment strategy. Each image contains 2 tumors, with the one on the animal's left side irradiated and that on its right side unirradiated. **B,** Changes to R_1 (= $1/T_1$) at different periods after carbon-ion irradiation. * $P < 0.05$ (irradiated vs unirradiated) for 2-way ANOVA with Bonferroni correction. MR, magnetic resonance; MTPL, multimodal thermosensitive polymer-modified liposome.

axis) × (depth) × $\pi/6$. The initial tumor volumes were controlled to be between 100 and 200 mm^3. Changes to the tumor volume were measured for 8 days after the treatments were applied.

Histological evaluation. The 15 mice of group B were used for immunohistological evaluation. All of the mice were euthanized and the tumors were extracted and prepared for histological evaluation with 4% paraformaldehyde followed by embedding in paraffin. Sections (3 μm thick) were stained immunohistochemically with Ki-67 as an early marker for proliferating tumor cells. All slides were examined with light microscopy (BZ-9000, KEYENCE, Osaka, Japan). Over 1000 Ki-67–positive and Ki-67–negative cells were counted using Image-J (National Institute of Health, Md.) and the fraction of the positive cells was calculated.

Statistical analysis. Signal intensities after carbon-ion irradiation, MTPL accumulation, and heating and the relative tumor volumes for each treatment strategy were compared using 2-way ANOVA with Bonferroni correction (Prism, ver.5, GraphPad software, Inc., La Jolla, Calif.). The fractions of Ki-67–positive cells were compared using 1-way ANOVA with Dunn correction. A significance level of 0.05 was used for all analysis.

RESULTS

Fig 2*A* presents typical MR images at 12 hours after carbon-ion irradiation of tumor on the left side. The MR signal intensities from the MTPL-administered mice are clearly higher than those from the animals without MTPL administration. In addition, MTPL administration

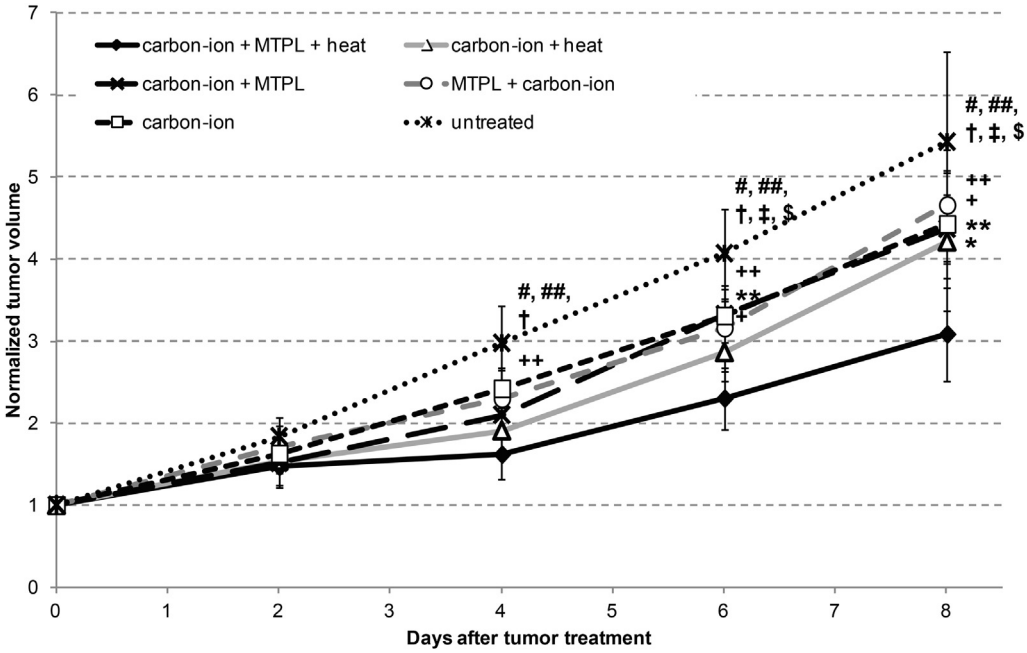

Fig 3. Longitudinal changes to the normalized tumor size. The treatment was applied on day 0, and tumor volume was monitored for 8 days after that. The error bars denote the standard deviation across animals receiving the same treatment. The level of significance was $P < 0.05$ for 2-way ANOVA with Bonferroni correction. Significant differences were observed for: *, "carbon-ion + MTPL + heat" vs "carbon-ion + heat;" **, "carbon-ion + MTPL + heat" vs "carbon-ion + MTPL;" +, "carbon-ion + MTPL + heat" vs "MTPL + carbon-ion;" ++, "carbon-ion + MTPL + heat" vs "carbon-ion;" #, "carbon-ion + MTPL + heat" vs "untreated;" ##, "carbon-ion + heat" vs "untreated;" †, "carbon-ion + MTPL" vs "untreated"; ‡, "MTPL + carbon-ion" vs "untreated"; and $, "carbon-ion" vs "untreated." MTPL, multimodal thermosensitive polymer-modified liposome.

induced MR signal changes in both the irradiated and unirradiated tumors. The "carbon-ion" only strategy did not affect the MR signal intensity at 12 hours after irradiation. The signal from the tumor on the carbon ion–irradiated side for the "carbon-ion + MTPL + heat" strategy increased more than that from the unirradiated tumor. Fig 2*B* quantifies the changes to the relaxation rate R_1 ($= 1/T_1$) for each treatment strategy. The R_1 for the "carbon-ion + MTPL + heat" strategy at 12 hours after carbon-ion irradiation was significantly higher than for the unirradiated tumor ($P < 0.05$). There were no significant differences between the R_1s of the irradiated and unirradiated tumors except for the "carbon-ion + MTPL + heat" strategy (Fig 2*B*).

Fig 3 compares the tumor growth over 1 week for all treatment strategies. The normalized tumor volume of the "carbon-ion + MTPL + heat" strategy was significantly smaller than those of the "untreated" and "carbon-ion" groups from day 4 to day 8, those of the "carbon-ion + MTPL" and "MTPL + carbon-ion" strategies from day 6 to day 8, and those of the "carbon-ion + heating" strategies on day 8. The normalized tumor volumes of the "carbon-ion + heat" and "carbon-ion + MTPL" strategies were significantly smaller than that of the "untreated" group from day 4 to day 8, and those of the "MTPL + carbon-ion" and "carbon-ion" strategies were also smaller than that of the "untreated" group from day 6 to day 8. On the other hand, the normalized tumor volume of the "carbon-ion + MTPL" strategy did not show any significant difference in comparison to that of the "MTPL + carbon-ion" strategy until day 8.

The immunohistological evaluation was performed as shown in Fig 4. Typical Ki-67–stained images are shown in Fig 4*A*. The fractions of positive cells for the treated groups were smaller than that of the untreated group. The average fraction of Ki-67–positive cells is presented in Fig 4*B*. The fraction of Ki-67–positive cells for the "carbon-ion + MTPL + heat" strategy is the smallest among all treatment groups and significantly lower than those of the "carbon-ion + MTPL," "carbon-ion," and "untreated" strategies.

DISCUSSION

This paper evaluated a combination treatment of high LET irradiation and a thermo-triggered liposomal DDS. Accumulation of the nanocarriers, MTPLs, in the tumor was not affected by whether the carbon-ion was

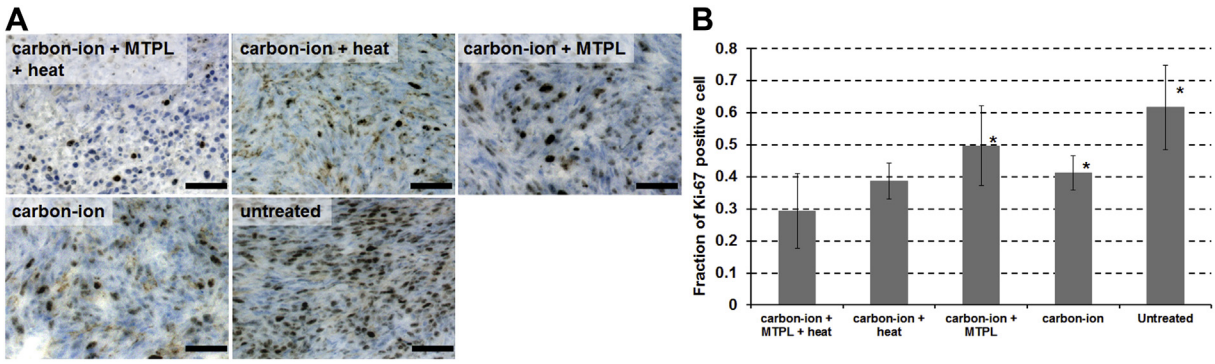

Fig 4. Histological evaluation at day 2 after treatment. (**A**) Typical Ki-67 images (Bar: 50 μm) and (**B**) the fraction of Ki-67 positive cells for various treatment strategies. The level of significance was $P < 0.05$ for one-way ANOVA with Dunn correction. MTPL, multimodal thermosensitive polymer-modified liposome.

irradiated before or after administration. Thermosensitivity was also unaffected, and the MR signal after MTPL administration and heating at the carbon-ion irradiated site was significantly higher than the signal from the control treatment strategies. Treatment with MTPLs, carbon-ion irradiation, and heating was significantly more effective than any of the other treatment strategies for at least 8 days after irradiation.

MTPL accumulation and perfusion assessment. Previous evaluation of MTPL kinetics in tumor without irradiation indicated that accumulation in the tumor region occurred for at least 12 hours after MTPL administration.[30] MR imaging to evaluate MTPL accumulation in the tumor region after irradiation was thus performed at 12 hours after treatment. As shown in Fig 2, the signal and R_1 at the irradiated site for both the "carbon-ion + MTPL" and "MTPL + carbon-ion" strategies showed no significant differences from those of the unirradiated contralateral tumor site.

It is known from studies on several animal tumor models that the vascular structure and function can change within 24 hours after a single-dose of x-ray irradiation.[42-54] On the other hand, in a previous study 20 Gy radiation applied to the colon-26 tumor model did not damage the microvessel structure and vascular endothelial cells at 24 hours, and there was no necrotic or inflammatory alteration in the tumor.[55] The vascular volume changes up until 24 hours after the irradiation, and the irradiated dose necessary to increase or decrease the volume varies depending on the tumor type and conditions.[42-46] Doses of 2.5 and 5 Gy have been reported to slightly increase the intravascular volume,[43,44] other studies have found that irradiation with 4–20 Gy decreases the volume,[42,43,45] while in another case the vascular volume increased for at least 24 hours after irradiation with 10 and 20 Gy.[46] Blood perfusion after irradiation with 5–20 Gy has been found to increase for at least 24 hours.[47-50] Some reports have found that the perfusion ratio decreased at 24 hours after irradiation, but the blood flow in the tumor did not diminish.[51,52] Vascular permeability and extravasation increased after irradiation with over 2.5 Gy.[42-44,53,54] In this article, the carbon-ion irradiation dose was 5 Gy, which means that the equivalent x-ray dose could be around 10 Gy because the relative biological effectiveness of carbon is around 2.0. Thus, local changes to the vasculature in the irradiated tumor will occur around 24 hours after irradiation. The MTPL was administered immediately after the irradiation and half-life in the bloodstream of the MTPL is approximately 6 hours. Thus, most of the injected MTPLs that accumulated in the tumor did so before the vessel alteration occurred. Also, the R_1 map calculated from the MRI indicates that the accumulation of MTPLs at the irradiated tumor site had a similar level to that of the contralateral unirradiated tumor. All the evidence suggests that accumulation of the MTPLs is not influenced by irradiation at the doses and time-point used.

Treatment effects. Tumor growth for the "carbon-ion + MTPL + heat" treatment was significantly slower than the growth observed for the other treatment strategies (Fig 3). Each of the carbon-ion irradiation strategies (ie "carbon-ion + MTPL", "MTPL + carbon-ion" and "carbon-ion + heat"), demonstrated some significant treatment effect in comparison with the "untreated" strategy as shown in Fig 3. However, histological evaluation found that the fraction of Ki-67 positive cells for the "carbon-ion + MTPL + heat" strategy was the smallest of all treatment strategies, which is consistent with the decreased rate of tumor growth for the "carbon-ion + MTPL + heat" strategy in Fig 4. The slower growth rate for the "carbon-ion + MTPL + heat" strategy might arise from a combination of the effects of DOX, high-LET beam irradiation and triggered heating.

Doxorubicin inhibits DNA and RNA polymerase resynthesis.[56] In this experiment, the DOX was released from the MTPLs in the tumor region after heating, so it would be expected that the treatment effects would be increased for the strategies that combined MTPLs and heating. A high-LET carbon-ion can directly induce double-strand breaks in DNA. DOX also has the potential to inhibit DNA reassociation, which interferes with the repair of DNA damaged by high-LET beam irradiation. It is therefore thought that the treatment effect of the "carbon-ion + MTPL + heat" strategy was generally higher than those of the other treatment groups. MTPLs that were not heated did not release the DOX; hence, the treatment effect expected from DOX decreased. Thus, the tumor growths of the "carbon-ion + MTPL" and "MTPL + carbon-ion" strategies were not significantly different from the growth of the "carbon-ion" strategy. The tumor growth of the "carbon-ion + heat" strategy was a little slower than those of the strategies that did not include the heating procedure. The temperature inside the tumor was monitored using a thermocouple probe to control the temperature at around 42.5°C. The heating duration was also relatively short (10 min.) compared with hyperthermia treatment. However, it is possible that the temperature in some parts of the tumor might be over 42.5°C, and therefore the benefit of heating alone might contaminate the therapeutic effect.

To simplify our protocol, the treatments including carbon-ion irradiation and MTPL administration were performed only once. Although tumor volume increased from day 6 after the full combination therapy ("carbon-ion + MTPL + heat"; Fig 3), the therapeutic effects were still significant in comparison to the other strategies. Clinical radiotherapy using a carbon-ion is usually performed multiple times to obtain the most effective therapeutic performance.[14,34,57,58] Also, in other clinical trials and preclinical studies, anticancer drugs were administered periodically.[23,26,27,36,59] Thus, multiple applications of the combined carbon-ion irradiation and MTPL administration treatment would improve the effectiveness in suppressing tumor growth. Also, if the MTPLs including suitable therapeutic radioisotopes such as ^{177}Lu or ^{90}Y are developed, the treatment effects will increase.

In future work, longitudinal treatment evaluation with multiple carbon-ion irradiations and drug administrations will be performed with additional microvascular evaluation, such as investigation of the vascular endothelial cells using CD31 antigen.

In conclusion, we have evaluated a combination of carbon-ion irradiation and thermo-triggered liposomal DDS therapy that significantly enhanced treatment efficacy. The MR-visible MTPL nanocarriers accumulated in the tumor region regardless of whether carbon-ion irradiation was applied or not, and tumor growth was significantly retarded in comparison with the control treatment strategies. Our combination strategy using carbon-ion beam irradiation and MTPLs provided effective treatment.

ACKNOWLEDGMENT

Conflicts of Interest: All authors have read the journal's policy on disclosure of potential conflicts of interest and have none to declare.

This research was mainly supported by an internal grant of the NIRS, and partly supported by the Center of Innovation Program (COI stream from JST) and Kakenhi Grants (#23700589, #24300167 and #17H00860). The authors thank Sayaka Shibata, Aiko Sekita and Chinami Kajiwara (NIRS) for help with animal experiments, and Dr. Atsushi Tsuji (NIRS) for invaluable advice. We are grateful to the staff of the HIMAC for their help with carbon-ion irradiation and to the Heavy-Ions at NIRS-HIMAC project for some financial support.

REFERENCES

1. Maas M, Beets-Tan RG, Lambregts DM, et al. Wait-and-see policy for clinical complete responders after chemoradiation for rectal cancer. J Clin Oncol 2011;29:4633–40.
2. Purdy JA. Intensity-modulated radiation therapy. Int J Radiat Oncol Biol Phys 1996;35:845–6.
3. Pirzkall A, Carol M, Lohr F, Hoss A, Wannenmacher M, Debus J. Comparison of intensity-modulated radiotherapy with conventional conformal radiotherapy for complex-shaped tumors. Int J Radiat Oncol Biol Phys 2000;48:1371–80.
4. Derycke S, Van Duyse B, De Gersem W, De Wagter C, De Neve W. Non-coplanar beam intensity modulation allows large dose escalation in stage III lung cancer. Radiother Oncol 1997; 45:253–61.
5. Choi Y, Kim JK, Lee HS, Hur WJ, Chai GY, Kang KM. Impact of intensity-modulated radiation therapy as a boost treatment on the lung-dose distributions for non-small-cell lung cancer. Int J Radiat Oncol Biol Phys 2005;63:683–9.
6. Kestin LL, Sharpe MB, Frazier RC, et al. Intensity modulation to improve dose uniformity with tangential breast radiotherapy: initial clinical experience. Int J Radiat Oncol Biol Phys 2000; 48:1559–68.
7. Evans PM, Donovan EM, Partridge M, et al. The delivery of intensity modulated radiotherapy to the breast using multiple static fields. Radiother Oncol 2000;57:79–89.
8. Vicini FA, Sharpe M, Kestin L, et al. Optimizing breast cancer treatment efficacy with intensity-modulated radiotherapy. Int J Radiat Oncol Biol Phys 2002;54:1336–44.
9. Damen EM, Brugmans MJ, van der Horst A, et al. Planning, computer optimization, and dosimetric verification of a segmented irradiation technique for prostate cancer. Int J Radiat Oncol Biol Phys 2001;49:1183–95.
10. Bos LJ, van der Geer J, van Herk M, Mijnheer BJ, Lebesque JV, Damen EM. The sensitivity of dose distributions for organ motion and set-up uncertainties in prostate IMRT. Radiother Oncol 2005; 76:18–26.

11. Tsujii H, Kamada T. A review of update clinical results of carbon ion radiotherapy. Jpn J Clin Oncol 2012;42:670–85.
12. Holley WR, Chatterjee A, Magee JL. Production of DNA strand breaks by direct effects of heavy charged particles. Radiat Res 1990;121:161–8.
13. Okada T, Kamada T, Tsuji H, et al. Carbon ion radiotherapy: clinical experiences at National institute of Radiological Science (NIRS). J Radiat Res 2010;51:355–64.
14. Miyamoto T, Yamamoto N, Nishimura H, et al. Carbon ion radiotherapy for stage I non-small cell lung cancer. Radiother Oncol 2003;66:127–40.
15. Mizoe JE, Hasegawa A, Jingu K, et al. Results of carbon ion radiotherapy for head and neck cancer. Radiother Oncol 2012; 103:32–7.
16. Yanagi T, Mizoe JE, Hasegawa A, et al. Mucosal malignant melanoma of the head and neck treated by carbon ion radiotherapy. Int J Radiat Oncol Biol Phys 2009;74:15–20.
17. Ishikawa H, Tsuji H, Kamada T, et al. Carbon-ion radiation therapy for prostate cancer. Int J Urol 2012;19:296–305.
18. Shinoto MYS, Terashima K, Yasuda S, et al. Carbon ion radiation therapy with concurrent Gemcitabine for patients with locally advanced pancreatic cancer. Int J Radiat Oncol Biol Phys 2016; 95:498–504.
19. Peer D, Karp JM, Hong S, Farokhzad OC, Margalit R, Langer R. Nanocarriers as an emerging platform for cancer therapy. Nat Nanotechnol 2007;2:751–60.
20. Torchilin VP. Recent advances with liposomes as pharmaceutical carriers. Nat Rev Drug Discov 2005;4:145–60.
21. Matsumura Y, Maeda H. A new concept for macromolecular therapeutics in cancer chemotherapy: mechanism of tumoritropic accumulation of proteins and the antitumor agent smancs. Cancer Res 1986;46:6387–92.
22. Nishiyama N, Kataoka K. Preparation and characterization of size-controlled polymeric micelle containing cis-dichlorodiammineplatinum(II) in the core. J Control Release 2001;74:83–94.
23. Plummer R, Wilson RH, Calvert H, et al. A Phase I clinical study of cisplatin-incorporated polymeric micelles (NC-6004) in patients with solid tumours. Br J Cancer 2011;104:593–8.
24. Hamaguchi T, Matsumura Y, Suzuki M, et al. NK105, a paclitaxel-incorporating micellar nanoparticle formulation, can extend in vivo antitumour activity and reduce the neurotoxicity of paclitaxel. Br J Cancer 2005;92:1240–6.
25. Hamaguchi T, Kato K, Yasui H, et al. A phase I and pharmacokinetic study of NK105, a paclitaxel-incorporating micellar nanoparticle formulation. Br J Cancer 2007;97:170–6.
26. Batrakova EV, Dorodnych TY, Klinskii EY, et al. Anthracycline antibiotics non-covalently incorporated into the block copolymer micelles: in vivo evaluation of anti-cancer activity. Br J Cancer 1996;74:1545–52.
27. Takahashi A, Yamamoto Y, Yasunaga M, et al. NC-6300, an epirubicin-incorporating micelle, extends the antitumor effect and reduces the cardiotoxicity of epirubicin. Cancer Sci 2013; 104:920–5.
28. Kaida S, Cabral H, Kumagai M, et al. Visible drug delivery by supramolecular nanocarriers directing to single-platformed diagnosis and therapy of pancreatic tumor model. Cancer Res 2010;70:7031–41.
29. Kono K, Nakashima S, Kokuryo D, et al. Multi-functional liposomes having temperature-triggered release and magnetic resonance imaging for tumor-specific chemotherapy. Biomaterials 2011;32:1387–95.
30. Kokuryo D, Nakashima S, Ozaki F, et al. Evaluation of thermo-triggered drug release in intramuscular-transplanted tumors using thermosensitive polymer-modified liposomes and MRI. Nanomedicine 2015;11:229–38.
31. Maeda A, DaCosta RS. Optimization of the dorsal skinfold window chamber model and multi-parametric characterization of tumor-associated vasculature. Intravital 2014;3:e27935.
32. Hak S, Helgesen E, Hektoen HH, et al. The effect of nanoparticle polyethylene glycol surface density on ligand-directed tumor targeting studied in vivo by dual modality imaging. ACS Nano 2012;6:5648–58.
33. Harrington KJ, Rowlinson-Busza G, Syrigos KN, et al. Pegylated liposome-encapsulated doxorubicin and cisplatin enhance the effect of radiotherapy in a tumor xenograft model. Clin Cancer Res 2000;6:4939–49.
34. Davies Cde L, Lundstrom LM, Frengen J, et al. Radiation improves the distribution and uptake of liposomal doxorubicin (caelyx) in human osteosarcoma xenografts. Cancer Res 2004; 64:547–53.
35. Dipetrillo T, Milas L, Evans D, et al. Paclitaxel poliglumex (PPX-Xyotax) and concurrent radiation for esophageal and gastric cancer: a phase I study. Am J Clin Oncol 2006;29:376–9.
36. Lammers T, Subr V, Peschke P, et al. Image-guided and passively tumour-targeted polymeric nanomedicines for radiochemotherapy. Br J Cancer 2008;99:900–10.
37. Senavirathna LK, Fernando R, Maples D, Zheng Y, Polf JC, Ranjan A. Tumor spheroids as an in vitro model for determining the therapeutic response to proton beam radiotherapy and thermally sensitive nanocarriers. Theranostics 2013;3:687–91.
38. Fernando R, Maples D, Senavirathna LK, et al. Hyperthermia sensitization and proton beam triggered liposomal drug release for targeted tumor therapy. Pharm Res 2014;31:3120–6.
39. Kono K, Ozawa T, Yoshida T, et al. Highly temperature-sensitive liposomes based on a thermosensitive block copolymer for tumor-specific chemotherapy. Biomaterials 2010;31:7096–105.
40. Aoki I, Yoneyama M, Hirose J, et al. Thermoactivatable polymer-grafted liposomes for low-invasive image-guided chemotherapy. Translational Res 2015;166:660–673.e1.
41. Kanai T, Endo M, Minohara S, et al. Biophysical characteristics of HIMAC clinical irradiation system for heavy-ion radiation therapy. Int J Radiat Oncol Biol Phys 1999;44:201–10.
42. Kalofonos H, Rowlinson G, Epenetos AA. Enhancement of monoclonal antibody uptake in human colon tumor xenografts following irradiation. Cancer Res 1990;50:159–63.
43. Wong HH, Song CW, Levitt SH. Early changes in the functional vasculature of Walker carcinoma 256 following irradiation. Radiology 1973;108:429–34.
44. Song CW, Sung JH, Clement JJ, Levitt SH. Vascular changes in neuroblastoma of mice following x-irradiation. Cancer Res 1974;34:2344–50.
45. Hilmas DE, Gillette EL. Microvasculature of C3H/Bi mouse mammary tumors after x-irradiation. Radiat Res 1975;61:128–43.
46. Clement JJ, Song CW, Levitt SH. Changes in functional vascularity and cell number following x-irradiation of a murine carcinoma. Int J Radiat Oncol Biol Phys 1976;1:671–8.
47. Bussink J, Kaanders JH, Rijken PF, Raleigh JA, Van der Kogel AJ. Changes in blood perfusion and hypoxia after irradiation of a human squamous cell carcinoma xenograft tumor line. Radiat Res 2000;153:398–404.
48. Dewhirst MW, Oliver R, Tso CY, Gustafson C, Secomb T, Gross JF. Heterogeneity in tumor microvascular response to radiation. Int J Radiat Oncol Biol Phys 1990;18:559–68.
49. Fokas E, Hanze J, Kamlah F, et al. Irradiation-dependent effects on tumor perfusion and endogenous and exogenous hypoxia markers in an A549 xenograft model. Int J Radiat Oncol Biol Phys 2010;77:1500–8.

50. Tozer GM, Bhujwalla ZM, Griffiths JR, Maxwell RJ. Phosphorus-31 magnetic resonance spectroscopy and blood perfusion of the RIF-1 tumor following X-irradiation. Int J Radiat Oncol Biol Phys 1989;16:155–64.
51. Kallman RF, DeNardo GL, Stasch MJ. Blood flow in irradiated mouse sarcoma as determined by the clearance of xenon-133. Cancer Res 1972;32:483–90.
52. Emami B, Ten Haken RK, Nussbaum GH, Hughes WL. Effects of single-dose irradiation in tumor blood flow studied by 15O decay after proton activation in situ. Radiology 1981;141:207–9.
53. Song CW, Levitt SH. Vascular changes in Walker 256 carcinoma of rats following X irradiation. Radiology 1971;100:397–407.
54. Kobayashi H, Reijnders K, English S, et al. Application of a macromolecular contrast agent for detection of alterations of tumor vessel permeability induced by radiation. Clin Cancer Res 2004;10:7712–20.
55. Saito S, Hasegawa S, Sekita A, et al. Manganese-enhanced MRI reveals early-phase radiation-induced cell alterations in vivo. Cancer Res 2013;73:3216–24.
56. Nishimura T, Suzuki H, Muto K, Tanaka N. Mechanism of adriamycin resistance in a subline of mouse lymphoblastoma L5178Y cells. J Antibiot (Tokyo) 1979;32:518–22.
57. Schulz-Ertner D, Haberer T, Jakel O, et al. Radiotherapy for chordomas and low-grade chondrosarcomas of the skull base with carbon ions. Int J Radiat Oncol Biol Phys 2002;53:36–42.
58. Kamada T, Tsujii H, Tsuji H, et al. Efficacy and safety of carbon ion radiotherapy in bone and soft tissue sarcomas. J Clin Oncol 2002;20:4466–71.
59. Cabral H, Murakami M, Hojo H, et al. Targeted therapy of spontaneous murine pancreatic tumors by polymeric micelles prolongs survival and prevents peritoneal metastasis. Proc Natl Acad Sci U S A 2013;110:11397–402.